

Numerical solution of two dimensional stagnation flows of Micropolar fluids towards a shrinking sheet by using SOR Iterative Procedure

Mohammad Shafique^{1*}, Atif Nazir², Fatima Abbas³

¹Ex-AP, Department of Mathematics, Gomal University, D I Khan, Pakistan

²Mathematics Group Coordinator, Yanbu Industrial College, Yanbu, Saudi Arabia.

³Department of Mathematics, Gomal University, Dera Ismail Khan, Pakistan

*Current: Private Teaching in Mathematics, Toronto, Canada.

Abstract

In this paper, the problem of two dimensional stagnation flows of micropolar fluids towards a shrinking sheet has been solved numerically by SOR iterative procedure. The similarity transformations have been used to reduce the highly nonlinear partial differential equations of motion to ordinary differential equations. The resulting equations are then integrated by using appropriate numerical techniques. The results have been calculated on three different grid sizes to check the accuracy of the results. The numerical results have been obtained for various values of the parameter α . For $\alpha > 0$, the problem relates to the stagnation flow towards a stretching sheet. For $\alpha < 0$, the problem relates to the flow towards a shrinking sheet. Moreover, the results computed for micropolar case are found in good agreement with those obtained with the Newtonian results.

Keywords: Micropolar Fluids; Shrinking Sheet and SOR Iterative Procedure.

1. Introduction

The flows about stretching phenomena have attracted the attention of numerous researchers yet work on the flow problems due to shrinking phenomena are limited. Mahapatra and Gupta [2, 3] combined both the stagnation point flow and stretching surface. Shafique and Rashid [4] examined the three dimensional fluid motion caused by the stretching of a flat surface. Ishak et al [5] analyzed the mixed convection boundary layers in the stagnation point flow toward a stretching vertical sheet. Flow of an electrically conducting non-Newtonian fluid past a stretching surface was studied by Able et al [6] when a uniform magnetic field acts transverse to the surface. Ishak et al [7] investigated the steady two-dimensional MHD stagnation flow towards a stretching sheet with variable surface temperature and obtained numerical results using the Keller-box method.

The MHD boundary layer flow of fluid over a shrinking sheet has been studied by Hayat et al [8] and Fang [9]. Nadeem et al [10] and Ara et al [11] have been investigated MHD boundary layer flow of fluid over an exponentially permeable shrinking sheet. The steady boundary layer flow and steady two-dimensional flow of a nanofluid past a nonlinearly permeable stretching/ shrinking sheet is numerically studied by Zaimi et al [12, 13]. Sajid and Hayat [14] applied homotopy analysis method for MHD viscous flow due to a shrinking sheet. The problem of [14] is studied by Noor et al. [15] by using simple non-perturbative method. Wang [16] considered two dimensional stagnation flows towards a shrinking sheet.

Eringen [1] offered the theory of micropolar fluids, a subclass of microfluids and established constitutive equations for fluids with micro-structure. This theory included the micro-rotational effects, micro-rotational inertia and couple stresses in addition to the usual stresses in the fluid medium. Recently, Shafique et al [17] have been studied the problem numerical solutions of MHD viscous flow of micropolar fluids due to a shrinking sheet numerically by using SOR iterative procedure.

In this work, the problem of the two dimensional stagnation flow of micropolar fluid towards a shrinking sheet is considered. The governing partial differential equations are reduced to ordinary differential form by using similarity transformations. The resulting equations have been solved numerically by using different numerical techniques namely SOR method and Simpson's (1/3) rule with the formula of Adams-Moulton. The numerical results have been obtained for various values of the parameter α and the Prandtl number Pr . For positive values of α , the problem relates to the stagnation flow towards a stretching sheet. For negative values of α , the problem relates to the flow towards a shrinking sheet.

2. Mathematical Analysis

The micropolar fluids flow is assumed to be steady, laminar and incompressible. The body force, the body couples and the viscous dissipation are neglected. The equations of motion for micropolar fluids flow have been considered for this problem:

$$\nabla \cdot \underline{V} = 0, \quad (1)$$

$$\kappa(\nabla \times \underline{\omega}) - (\mu + \kappa)\nabla \times (\nabla \times \underline{V}) - \nabla \pi = \rho(\underline{V} \cdot \nabla) \underline{V}, \quad (2)$$

$$(\alpha + \beta + \gamma) \nabla \cdot (\nabla \times \underline{\omega}) - \gamma (\nabla \times \nabla \times \underline{\omega}) + \kappa(\nabla \times \underline{V}) - 2\kappa \underline{\omega} = \rho j(\underline{V} \cdot \nabla) \underline{\omega}, \quad (3)$$

$$\rho C_p (\underline{V} \cdot \nabla) T = K \nabla^2 T. \quad (4)$$

where ρ is the density, \underline{V} is the velocity vector, $\underline{\omega}$ is the micro-rotation or spin vector and π is the pressure respectively. The j is micro-inertia, α , β , γ , μ , λ and κ are material constants. The dissipation function is Φ while T , C_p and K are fluid temperature, specific heat and heat conductivity respectively.

The equations of motion for micropolar fluids have been considered for this problem with the following assumptions:

- i) The two dimensional potential stagnation flow at infinity is given by $u = ax$, $w = -az$ where a is the strength of the stagnation flow.
- ii) The velocity components, on the stretching surface are $u = b(x + c)$, $w = 0$ where b is stretching rate and $b < 0$ indicates the shrinking of the surface. The stretching origin is located at $-c$.
- iii) T_w represents the constant temperature of the surface of the tube and T_∞ denotes the temperature of ambient fluid where $T_w > T_\infty$.

The set of equations (1) to (4) can be written by using the velocity vector $\underline{V} = (u(x, z), 0, w(x, z))$ and spin vector $\underline{\omega} = \omega(0, \omega_2(x, z), 0)$. The resulting partial differential equations, with the above assumptions, become:

$$\frac{\partial u}{\partial x} + \frac{\partial w}{\partial z} = 0, \quad (5)$$

$$(\mu + \kappa) \left(\frac{\partial^2 u}{\partial x^2} + \frac{\partial^2 u}{\partial z^2} \right) - \kappa \frac{\partial \omega_2}{\partial z} - \frac{\partial \pi}{\partial x} = \rho \left(u \frac{\partial u}{\partial x} + w \frac{\partial u}{\partial z} \right), \quad (6)$$

$$(\mu + \kappa) \left(\frac{\partial^2 w}{\partial x^2} + \frac{\partial^2 w}{\partial z^2} \right) + \kappa \frac{\partial \omega_2}{\partial x} - \frac{\partial \pi}{\partial z} = \rho \left(u \frac{\partial w}{\partial x} + w \frac{\partial w}{\partial z} \right), \quad (7)$$

$$\gamma \left(\frac{\partial^2 \omega_2}{\partial x^2} + \frac{\partial^2 \omega_2}{\partial z^2} \right) + \kappa \left(\frac{\partial u}{\partial z} - \frac{\partial w}{\partial x} \right) - 2\kappa \omega_2 = \rho j \left(u \frac{\partial \omega_2}{\partial x} + w \frac{\partial \omega_2}{\partial z} \right), \quad (8)$$

$$\rho C_p \left(u \frac{\partial T}{\partial x} + w \frac{\partial T}{\partial z} \right) = K \left(\frac{\partial^2 T}{\partial x^2} + \frac{\partial^2 T}{\partial z^2} \right). \quad (9)$$

The following similarity transformations are used to obtain the partial differential equations (5) to (9) in ordinary differential form

$$u = axf'(\eta) + bcg(\eta), w = -\sqrt{av}f(\eta), \omega_2 = \sqrt{a/v}(axL(\eta) + bcM(\eta)), \theta(\eta) = \frac{T - T_\infty}{T_0 - T_w}, \quad (10)$$

where $\eta = \sqrt{\frac{a}{\nu}} z$ is a non dimensional variable.

The equation of continuity (5) is satisfied. The equations (6), (8) and (9) by using (10) lead to:

$$f''' - C_1 L' + 1 = f'^2 - f'' f, \quad (11)$$

$$g'' - C_1 M' = g f' - g' f, \quad (12)$$

$$L'' + C_2 (f'' - 2L) = C_3 (f L - f L'), \quad (13)$$

$$M'' + C_2 (g' - 2M) = C_3 (g L - f M'), \quad (14)$$

$$\theta'' + \text{Pr} f \theta' = 0. \quad (15)$$

Here $C_1 = \frac{\kappa}{\mu + \kappa}$, $C_2 = \frac{\kappa \nu}{\gamma a}$ and $C_3 = \frac{\rho j \nu}{\gamma}$. are dimensionless constants.

The boundary conditions are:

$$\begin{cases} f = 0, & f' = \alpha, & g = 1, & L = 0, & M = 0, & \theta = 1, & \text{at } \eta = 0, \\ f' \rightarrow 1, & g \rightarrow 0, & L \rightarrow 0, & M \rightarrow 0, & \theta \rightarrow 0, & & \text{as } \eta \rightarrow \infty. \end{cases} \quad (16)$$

Where $\alpha = \frac{b}{a}$, $\text{Pr} = \frac{\rho \nu C_p}{K}$ and $\nu = \frac{\mu}{\rho}$ is the coefficient of kinematics viscosity. The prime denotes the differentiation with respect to η .

3. Finite Difference Equations

In order to solve the equations (11) to (15) numerically, we set

$$P = f'. \quad (17)$$

Then equations (11) to (15) become:

$$P'' - C_1 L' + 1 = P^2 - P' f, \quad (18)$$

$$g'' - C_1 M' = g P - g' f, \quad (19)$$

$$L'' + C_2 (P' - 2L) = C_3 (P L - f L'), \quad (20)$$

$$M'' + C_2 (g' - 2M) = C_3 (g L - f M'), \quad (21)$$

$$\theta'' + \text{Pr} f \theta' = 0. \quad (22)$$

The boundary conditions (16) become:

$$\begin{cases} f = 0, & P = \alpha, & g = 1, & L = 0, & M = 0, & \theta = 1, & \text{at } \eta = 0, \\ P \rightarrow 1, & g \rightarrow 0, & L \rightarrow 0, & M \rightarrow 0, & \theta \rightarrow 0, & & \text{as } \eta \rightarrow \infty. \end{cases} \quad (23)$$

We now approximate the derivatives in equations (18) to (22) by central-difference approximations at a typical grid point $\eta = \eta_n$ of the interval $[0, \infty)$ and we obtain

$$(2 + h f_n) P_{n+1} + (2 - h f_n) P_{n-1} + 2h^2 - C_1 (L_{n+1} - L_{n-1}) - (4 + 2h^2 P_n) P_n = 0, \quad (24)$$

$$(2 + h f_n) g_{n+1} + (2 - h f_n) g_{n-1} - C_1 h (M_{n+1} - M_{n-1}) - (4 + 2h^2 P_n) g_n = 0, \quad (25)$$

$$(2 + C_3 h f_n) L_{n+1} + (2 - C_3 h f_n) L_{n-1} + C_2 h (P_{n+1} - P_{n-1}) = (4 + C_2 4h^2 + C_3 2h^2 P_n) L_n, \quad (26)$$

$$(2 + C_3 h f_n) M_{n+1} + (2 - C_3 h f_n) M_{n-1} - C_2 h (g_{n+1} - g_{n-1}) = 2h^2 C_3 g_n L_n + (4 + C_2 4h^2) M_n, \quad (28)$$

$$2(\theta_{n+1} + \theta_{n-1}) + \text{Pr} f_n h (\theta_{n+1} - \theta_{n-1}) = 4\theta_n, \quad (29)$$

where h denotes a grid size and $f_n = f(\eta_n)$, $g_n = g(\eta_n)$, $P_n = P(\eta_n)$, $L_n = L(\eta_n)$, $M_n = M(\eta_n)$ and $\theta_n = \theta(\eta_n)$. For computational purpose, we shall replace the interval $[0, \infty)$ by $[0, \beta]$.

4. Computational Procedure

We now solve numerically the first order ordinary differential equation (17) and the system of finite difference equations (24) to (29) at each interior grid point of the interval. The equation (17) is integrated by the Simpson's (1/3) rule with the formula of Adams-Moulton where as the set of equations (24) to (29) are solved by using SOR iterative procedure subject to the appropriate conditions (23).

In order to accelerate the speed of convergence of the SOR iterative procedure, the optimum value of the relaxation parameter ω_{opt} is estimated between 1 and 2. The optimum value of the relaxation parameter for the problem under consideration is 1.5. The procedure is repeated until convergence is obtained according to the criterion $\max |U^{n+1} - U^n| < 10^{-6}$ where n denotes the number of iterations and U stands for each the functional value.

5. Discussion on Numerical Results

The solutions have been obtained for the values of parameter α in the range $-1.2475 \leq \alpha \leq 10$. This particular range of parameter α has been taken during computational work for the convergence of our numerical scheme. The computations have been made on different grid sizes namely $h=0.01, 0.005, 0.0025$ and then the results have been compared. The calculations have also been carried out for three sets of material constants C_1, C_2 and C_3 given in the table below.

Case	C_1	C_2	C_3
I	0.01	1.5	2.5
II	0.5	2.0	3.0
III	0.1	1.0	2.0

If the above constants are zero, the micropolar fluids flow becomes the Newtonian fluids flow. The three different cases for the values of the constants have been considered for this micropolar fluids flow problem during the computational work. When C_1 is small and C_2, C_3 are large, the micropolar fluids flow resembles with Newtonian fluids flow as in Case-I. The cases II and III are far from the results of Newtonian fluids due to fast micro rotation of the molecules because of large values of material constants.

The table 1 to 5 show the comparison of the values for the functions f, f', g, θ, L and M in the case-I of the material constants for each of grid sizes. The results compare very well and validate our computational procedure. Table 6 and 7 respectively show the difference of values of $f''(0)$ and $g'(0)$ for micropolar fluids and Newtonian fluids for different values of parameter α .

Graphically, the results for function $f(\eta)$ have been shown in Figure 1 and Figure 2. Figure 1 shows that $f(\eta)$ increases for positive values of α and for $\alpha = 0$, it behaves like Hiemenz [19] flow towards a solid plate. The function $f(\eta)$ is initially negative for negative values of α as shown in Figure 2. The Figure 3 demonstrates the effect of α on the non-alignment function g . It is noticed that the effect is large for $\alpha < 0$ and small for $\alpha \geq 0$. Figure 4 presents the behavior of $f''(0)$ for different values of α . Also, $g'(0)$ is plotted against α in Figure 5. The heat transfer rate $-\theta'(0)$ has been shown in Figure 6. The non-alignment function g does not affect the heat transfer rate. However, the heat transfer rate decreases by increasing the value of shrinking parameter α .

Consequently, the effects of different parameters are observed on the similarity, velocity, micro rotation, temperature profiles, skin friction coefficient $f''(0)$ and the Nusselt number $-\theta'(0)$. The function $f(\eta)$ increases for positive values of α and for $\alpha = 0$, it behaves like Hiemenz flow towards a solid plate. The effect is large for $\alpha < 0$ and small for $\alpha \geq 0$ on the non-alignment function g . For increasing values of the shrinking parameter α , the boundary layer thickness increases and hence the heat transfer rate decreases. The increasing values of α decrease the micro rotation.

Table 1: The functions f, f', g, θ, L and M in the case-I for $\alpha = 0.0$

h	η	f	f'	g	θ	L	M
0.010	0.000	0.000000	0.000000	1.000000	1.000000	0.000000	0.000000
	1.000	0.459306	0.778123	0.322544	0.518531	0.089956	-0.147857
	2.000	1.362290	0.973393	0.053132	0.172488	0.011674	-0.026603
	3.000	2.353045	0.998629	0.004081	0.032636	0.000519	-0.001483
	4.000	3.352836	1.000166	0.000134	0.003186	-0.000012	-0.000036
	5.000	4.352935	1.000000	0.000000	0.000000	0.000000	0.000000
0.005	0.000	0.000000	0.000000	1.000000	1.000000	0.000000	0.000000
	1.000	0.459426	0.778261	0.180611	0.276249	0.074642	-0.100637
	2.000	1.362506	0.973456	0.011288	0.030722	0.009942	-0.007279
	3.000	2.353212	0.998350	0.000260	0.001383	0.000499	-0.000114
	4.000	3.352648	0.999845	0.000002	0.000028	0.000017	-0.000001
	5.000	4.352568	1.000000	0.000000	0.000000	0.000000	0.000000
0.0025	0.000	0.000000	0.000000	1.000000	1.000000	0.000000	0.000000
	1.000	0.459463	0.778331	0.011918	0.031670	0.010694	-0.007802
	2.000	1.362593	0.973489	0.000003	0.000032	0.000119	-0.000001
	3.000	2.353304	0.998353	0.000000	0.000000	0.000008	0.000000
	4.000	3.352744	0.999851	0.000000	0.000000	0.000000	0.000000
	5.000	4.352669	1.000000	0.000000	0.000000	0.000000	0.000000

Table 2: The functions f, f', g, θ, L and M in the case-I for $\alpha = 5.0$

h	η	f	f'	g	θ	L	M
0.010	0.000	0.000000	5.000000	1.000000	1.000000	0.000000	0.000000
	1.000	2.370419	1.217495	0.069690	0.200459	-0.065634	-0.022749
	2.000	3.431093	1.005358	0.002150	0.019635	-0.001332	-0.000568
	3.000	4.432355	1.000168	0.000027	0.001003	-0.000013	-0.000006
	4.000	5.432520	1.000149	0.000000	0.000026	-0.000011	0.000000
	5.000	6.432594	1.000000	0.000000	0.000000	0.000000	0.000000
0.005	0.000	0.000000	5.000000	1.000000	1.000000	0.000000	0.000000
	1.000	2.370183	1.217371	0.030431	0.072562	-0.057457	-0.011102
	2.000	3.430825	1.005398	0.000177	0.001148	-0.001260	-0.000052
	3.000	4.432055	1.000035	0.000000	0.000006	-0.000002	0.000000
	4.000	5.432068	0.999973	0.000000	0.000000	-0.000005	0.000000
	5.000	6.432043	1.000000	0.000000	0.000000	0.000000	0.000000
0.0025	0.000	0.000000	5.000000	1.000000	1.000000	0.000000	0.000000
	1.000	2.369986	1.217291	0.000533	0.002287	-0.008753	-0.000196
	2.000	3.430595	1.005478	0.000000	0.000000	-0.000216	0.000000
	3.000	4.431884	1.000095	0.000000	0.000000	-0.000004	0.000000
	4.000	5.431927	1.000023	0.000000	0.000000	-0.000003	0.000000
	5.000	6.431950	1.000000	0.000000	0.000000	0.000000	0.000000

Table 3: The functions f, f', g, θ, L and M in the case-I for $\alpha = 10.0$

h	η	f	f'	g	θ	L	M
0.010	0.000	0.000000	0.000000	1.000000	1.000000	0.000000	0.000000
	1.000	0.459653	0.779236	0.320681	0.518518	0.097845	-0.161322
	2.000	1.363549	0.973893	0.051967	0.172441	0.011255	-0.025445
	3.000	2.354521	0.998681	0.003934	0.032611	0.000484	-0.001370
	4.000	3.354327	1.000163	0.000127	0.003181	-0.000016	-0.000034
	5.000	4.354425	1.000000	0.000000	0.000000	0.000000	0.000000
0.005	0.000	0.000000	0.000000	1.000000	1.000000	0.000000	0.000000
	1.000	0.459955	0.779438	0.151223	0.252036	0.076648	-0.099938

	2.000	1.363914	0.973906	0.006841	0.022212	0.009292	-0.004636
	3.000	2.354843	0.998473	0.000106	0.000702	0.000470	-0.000045
	4.000	3.354384	0.999920	0.000001	0.000009	0.000009	0.000000
	5.000	4.354332	1.000000	0.000000	0.000000	0.000000	0.000000
0.0025	0.000	0.000000	0.000000	1.000000	1.000000	0.000000	0.000000
	1.000	0.459991	0.779503	0.007319	0.023049	0.010161	-0.005105
	2.000	1.363997	0.973933	0.000001	0.000011	0.000128	0.000000
	3.000	2.354930	0.998476	0.000000	0.000000	0.000009	0.000000
	4.000	3.354476	0.999924	0.000000	0.000000	0.000000	0.000000
	5.000	4.354421	1.000000	0.000000	0.000000	0.000000	0.000000

Table 4: The functions f, f', g, θ, L and M in the case-I for $\alpha = -1.0$

h	η	f	f'	g	θ	L	M
0.010	0.000	0.000000	-1.000000	1.000000	1.000000	0.000000	0.000000
	1.000	-0.378246	0.171277	0.687523	0.751276	0.305010	-0.257099
	2.000	0.147493	0.784647	0.261014	0.444266	0.119435	-0.164678
	3.000	1.046748	0.968272	0.053380	0.171348	0.016082	-0.031767
	4.000	2.034839	0.997714	0.005137	0.035379	0.000867	-0.002144
	5.000	3.034231	1.000000	0.000000	0.000000	0.000000	0.000000
0.005	0.000	0.000000	-1.000000	1.000000	1.000000	0.000000	0.000000
	1.000	-0.378098	0.171665	0.325622	0.457318	0.192970	-0.193321
	2.000	0.148048	0.784970	0.024059	0.066473	0.042459	-0.023922
	3.000	1.047424	0.968260	0.000439	0.002029	0.006498	-0.000435
	4.000	2.035497	0.997627	0.000003	0.000019	0.000517	-0.000002
	5.000	3.034782	1.000000	0.000000	0.000000	0.000000	0.000000
0.0025	0.000	0.000000	-1.000000	1.000000	1.000000	0.000000	0.000000
	1.000	-0.378093	0.171733	0.025207	0.067957	0.044146	-0.025080
	2.000	0.148161	0.785074	0.000003	0.000023	0.000985	-0.000003
	3.000	1.047578	0.968253	0.000000	0.000000	0.000096	0.000000
	4.000	2.035643	0.997628	0.000000	0.000000	0.000009	0.000000
	5.000	3.034931	1.000000	0.000000	0.000000	0.000000	0.000000

Table 5: The functions f, f', g, θ, L and M in the case-I for $\alpha = -1.2475$

h	η	f	f'	g	θ	L	M
0.010	0.000	0.000000	-1.247500	1.000000	1.000000	0.000000	0.000000
	1.000	-0.879697	-0.473801	1.370493	0.923868	0.356071	-0.205766
	2.000	-0.955100	0.288294	1.034393	0.789403	0.315747	-0.388929
	3.000	-0.402366	0.762454	0.502578	0.542226	0.144336	-0.313651
	4.000	0.473554	0.952671	0.137096	0.227418	0.029867	-0.102519
	5.000	1.455968	1.000000	0.000000	0.000000	0.000000	0.000000
0.005	0.000	0.000000	-1.247500	1.000000	1.000000	0.000000	0.000000
	1.000	-0.886570	-0.486245	1.369960	0.899124	0.353995	-0.203845
	2.000	-0.976413	0.273679	1.035697	0.744089	0.318301	-0.387631
	3.000	-0.435777	0.753557	0.505280	0.494874	0.148930	-0.316298
	4.000	0.434516	0.949856	0.139091	0.203511	0.031905	-0.105730
	5.000	1.415766	1.000000	0.000000	0.000000	0.000000	0.000000
0.0025	0.000	0.000000	-1.247500	1.000000	1.000000	0.000000	0.000000
	1.000	-0.886605	-0.486269	1.036075	0.743939	0.318831	-0.387360
	2.000	-0.976382	0.273827	0.140380	0.204066	0.033406	-0.107411
	3.000	-0.435632	0.753583	0.000003	0.000006	0.000481	-0.000005
	4.000	0.434665	0.949843	0.000000	0.000000	0.000144	0.000000
	5.000	1.415906	1.000000	0.000000	0.000000	0.000000	0.000000

Table 6: The comparison of Micropolar fluids and Newtonian fluids for $f''(0)$

α	Micropolar fluids			Newtonian fluids	
	I	II	III	Present	Wang [16]
0	1.232052	12293181	1.2281510	1.230355	1.232588
0.1	1.1460781	1.437058	1.1422514	1.146591	1.14656
0.2	1.050842	1.0486781	1.0476827	1.051265	1.05113
0.5	0.711513	0.7117987	0.7112265	0.713372	0.71330
1.0	-0.000548	0.0000000	-0.0000715	-0.00007	0.0
2.0	-1.871812	-1.8830776	-1.8790721	-1.8854618	-1.88731
5.0	-10.237695	-10.229112	-10.221673	-10.239030	-10.26475
8.0	-21.526622	-21.597099	-21.595191	-21.610450	----
10.0	-30.535888	-38.525970	-30.514144	-30.164527	----
-0.05	1.269106	1.2683004	1.2671619	1.271822	----
-0.15	1.342022	1.3381242	1.3369202	1.342702	----
-0.25	1.401526	1.3975501	1.3952910	1.402199	1.40224
-0.50	1.492685	1.4894008	1.4867782	1.495576	1.49567
-0.75	1.486864	1.4806270	1.4771938	1.488662	1.48930
-1.0	1.325488	1.3162851	1.3104677	1.3282775	1.32882
-1.15	1.077223	1.0636806	1.0537624	1.0814666	1.08223
-1.2465	0.612164	0.6095290	0.6055672	0.6310463	0.55430
-1.2475	0.591516	0.5125523	0.3724575	0.6090641	----

Table 7: The comparison of Micropolar fluids and Newtonian fluids for $g'(0)$

α	Micropolar fluids			Newtonian fluids	
	I	II	III	Present	Wang [16]
0	-0.810277	-0.805786	-0.8032501	-0.8110881	-0.811301
0.1	-0.862044	-0.8577407	-0.8552611	-0.8629799	-0.86345
0.2	-0.911408	-0.9073198	-0.9049118	-0.9122908	-0.91330
0.5	-1.0481417	-1.0443150	-1.0422885	-1.0489881	-1.05239
1.0	-1.2472987	-1.249310	-1.2421429	-1.2480258	-1.25331
2.0	-1.578981	-1.5761196	-1.5748381	-1.5795648	-1.58957
5.0	-2.312821	-2.310741	-2.309847	-2.313268	-2.33810
8.0	-2.865297	-2.863574	-2.862859	-2.865630	----
10.0	-3.179693	-3.178179	-3.177577	-3.179997	----
-0.05	-0.783461	-0.7788777	-0.7763386	-0.7838547	----
-0.15	-0.727457	-0.7222116	-0.7200062	-0.7285535	----
-0.25	-0.668591	-0.6632447	-0.6598890	-0.6691158	-0.66857
-0.50	-0.502211	-0.4967153	-0.4927874	-0.5033791	-0.50145
-0.75	-0.29509	-0.2884805	-0.2838433	-0.2966404	-0.29376
-1.0	-0.001907	0.0067234	0.01418590	-0.004076	0.0
-1.15	0.296581	0.3095985	0.3225684	0.2933860	0.297995
-1.2465	0.869560	0.9513974	0.8028746	0.8562684	0.99904
-1.2475	0.894725	0.9725598	1.0902881	0.8745313	----

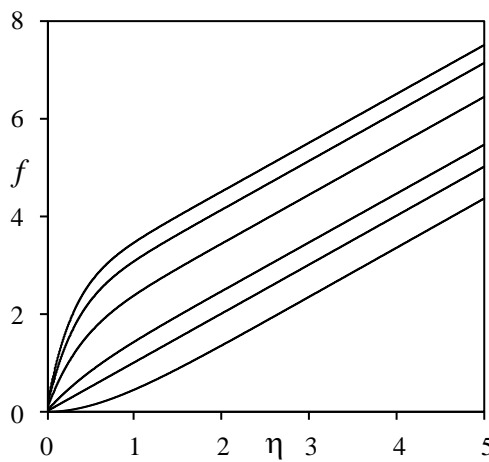


Figure 1: Graph of f for different values of $\alpha = 0, 1, 2, 5, 8$ and 10 from bottom.

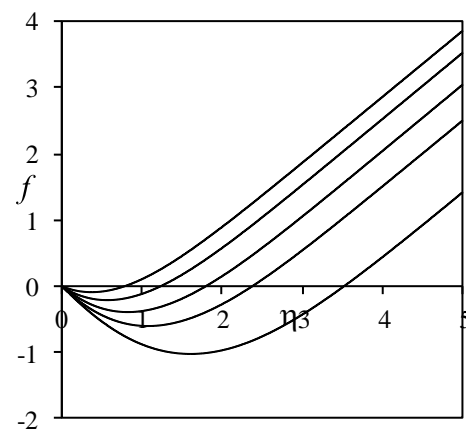


Figure 2: Graph of f for different values of $\alpha = -0.5, -0.75, -1, -1.15$ and -1.2475 from top

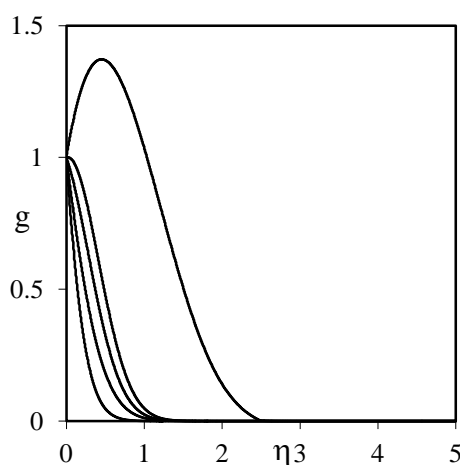


Figure 3: Graph of g for different values of $\alpha = 5, 0, -1, -1.15$ and -1.2475 from bottom.

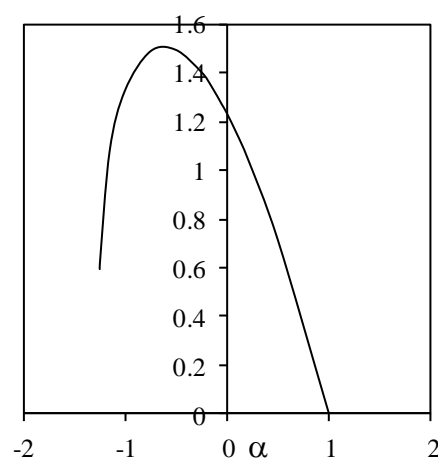


Figure 4: Graph of skin friction coefficient $f''(0)$

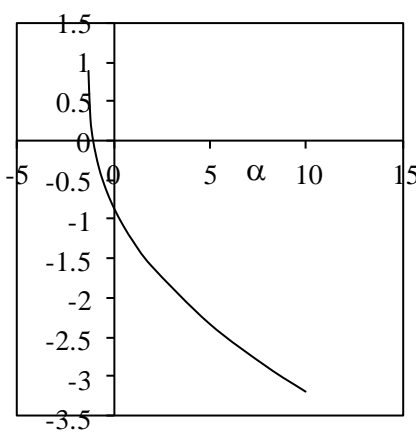


Figure 5: Graph of the gradient of non alignment function g i.e. $g'(0)$

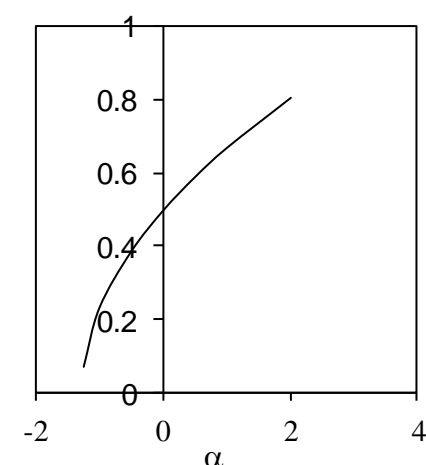


Figure 6: Graph of the heat transfer function $-θ'(0)$

References

- [1] Eringen, A.C. (1966). Theory of micropolar fluids. *J. Math. Mech.* 16, 1-18.
- [2] T. R. Mahaputra and A. S. Gupta, Heat transfer in stagnation-point flow towards a stretching surface, *Heat Mass Transfer*, 38(2004)811-820.
- [3] T. R. Mahaputra and A. S. Gupta, Stagnation-point flow towards a stretching surface, *Can. J. Chem. Engg.* 81(2003)258-263.
- [4] M. Shafique and A. Rashid, The numerical methods for the 3- dimensional flow due to a stretching flat surface *Int. J. of Applied Math.* 17(1) (2005) 15-26.
- [5] A. Ishak, R. Nazar and I. Pop, Mixed convection boundary layers in he stagnation point flow toward a stretching vertical sheet , *Meccanica* ,41(2006)509-518.
- [6] S. Able, P. H. Veena, K. Rajagopal and V. K. Pravin, non- Newtonian magnetohydrodynamic flow over a stretching surface with heat and mass transfer, *Int. J. Nonlinear Mech.* 39(2004)1067-1078.
- [7] A. Ishak, K. Jafar, R. Nazar and I. Pop, MHD stagnation point flow towards a stretching sheet, *Physica A* 388 (2009)3377-3383.
- [8] T. Hayat, Z. Abbas and M. Sajid, (2007), On the Analytic Solution of MHD Flow of a Second Grade Fluid Over a Shrinking Sheet, *J. Appl. Mech.* 74(6), 1165-1171
- [9] Tiegang Fang, (2008), Boundary layer flow over a shrinking sheet with power-law velocity, *International Journal of Heat and Mass Transfer*, Volume 51, Issues 25–26, 5838–5843.
- [10] S. Nadeem, Rizwan Ul Haq, C. Lee, (2012), MHD flow of a Casson fluid over an exponentially shrinking sheet,*Scientia Iranica B* 19 (6), 1550–1553.
- [11] Asmat Ara, Najeeb Alam Khan, Hassam Khan, Faqiha Sultan, (2014), Radiation effect on boundary layer flow of an Eyring–Powell fluid over an exponentially shrinking sheet, *Ain Shams Engineering Journal*, Volume 5, Issue 4, 1337–1342.
- [12] Khairy Zaimi, Anuar Ishak & Ioan Pop, (2014), Boundary layer flow and heat transfer over a nonlinearly permeable stretching/shrinking sheet in a nanofluid, *Scientific Reports*4, Article number:4404 doi:10.1038/srep04404.
- [13] Khairy Zaimi,, Anuar Ishak, Ioan Pop , (2014), Flow Past a Permeable Stretching/Shrinking Sheet in a Nanofluid Using Two-Phase Model, *PLoS ONE* 9(11): e111743.
- [14] Sajid, M. and Hayat, T., The application of homotopy analysis method for MHD viscous flow due to a shrinking sheet, *Chaos Solitons Fractals*, 39, (2009), 1317-1323.
- [15] Noor, N. F. M., Kechil, S. A. and Hashim, I., Simple non-perturbative solution for MHD viscous flow due to a shrinking sheet, *Commun Nonlinear Sci Numer Sim Ilat* 15, (2010),144-148.
- [16] Wang. C.Y. (2008), Stagnation flow towards a shrinking sheet, *International journal of Non-Linear Mechanics*, 43, 377 – 382.
- [17] M. Shafique , Fatima Abbas, A Rashid. MHD Viscous Flow of Micropolar Fluids due to a Shrinking Sheet. *International Journal of Emerging Technology and Advanced Engineering*, Volume 3, Issue 7, 651-658, 2013.
- [18] C. F. Gerald, “Applied Numerical Analysis,” Addison- Wesley Publication, New York, 1989.
- [19] Hiemenz, K. (1911), Die Grenzschicht an einem in den gleichformigen flussigkeits strom eingetauchten garden Kreiszylinder, *Dinglers Polytech. J.*, 326, 321-324.